The Oxetane Ring in Taxol

Minmin Wang, Ben Cornett, Jim Nettles, Dennis C. Liotta, and James P. Snyder*

Department of Chemistry, Emory University, Atlanta, Georgia 30322

Received October 14, 1999

Numerous structure−activity studies combining synthesis and bioassay have been performed for the anti-cancer drug Taxol. The four-membered D-ring, an oxetane, is one of four structural features regarded to be essential for biological activity. This proposition is examined by application of a Taxol−epothilone minireceptor, K_i estimation for microtubule binding and docking of Taxol analogues into a model of the Taxol−tubulin complex. In this way, we evaluate the two characteristics considered responsible for oxetane function: (1) rigidification of the tetracyclic Taxol core to provide an appropriate framework for presenting the C-2, C-4, C-13 side chains to the microtubule protein and (2) service as a hydrogen-bond acceptor. An energy decomposition analysis for a series of Taxol analogues demonstrates that the oxetane ring clearly operates by both mechanisms. However, a broader analysis of four-membered ring containing compounds, C- and D-seco derivatives, and structures with no oxetane equivalent underscores that the four-membered ring is not necessary for Taxol analogue bioactivity. Other functional groups and ligand−protein binding characteristics are fully capable of delivering Taxol biobehavior as effectively as the oxetane D-ring. This insight may contribute to the design and development of novel anticancer drugs.

Introduction

Taxol (**1**) isolated from the bark of *Taxus brevifolia* in the late 1960s,[1] and its semisynthetic congener, Taxotere[2] (**2**), have become the drugs of choice for the treatment of ovarian and breast cancer.[3] In attempts to understand the action of Taxol at its microtubule target, extensive SAR studies have been conducted. The main conclusions of these studies are that the C-13 side chain, the ester groups at C-2 and C-4, the oxetane ring, and the rigid core to which these moieties are attached are all essential for biological activity.

	R_1	R_2	
Taxol	Ph	Ac	**1**
Taxotere	t-BuO	H	**2**

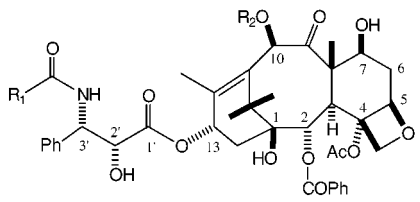

While a number of studies have pointed to "hydrophobic collapse" as the origin of the importance of the side chains to Taxol's bioaction,[4] the role of the oxetane ring has been more speculative. Two hypotheses have emerged. On one hand, the four-membered ring might operate to rigidify the Taxol core and thereby enforce a favorable conformational bias on the side chains at C-2, C-4, and C-13. Alternatively, the oxetane oxygen might exert an advantageous electrostatic force by participating in a hydrogen bond or an otherwise energy-lowering dipole−dipole interaction with the tubulin protein.

Three types of studies have addressed aspects of the oxetane question. First, the oxygen atoms in the four-membered rings of Taxol, Taxotere, and baccatin analogues have been replaced by nitrogen[5] and sulfur[6] heteroatoms. Second, both the C and D rings of Taxol have been ruptured to generate seco-analogues with varying degrees of activity.[7,8] Third, a number of active compounds with Taxol-like properties have been prepared that do not incorporate a four-membered ring as part of the rigid core.[9−11] In the present paper, we use the minireceptor approach[12,13] and a refined model of the Taxol−β-tubulin binding pocket[14] derived from the electron crystallography coordinates[15] to investigate the consequences of each of these synthetic manipulations

(1) (a) Wani, M. C.; Taylor, H. L.; Wall, M. E.; Coggon, P.; McPhail, A. T. *J. Am. Chem. Soc.* **1971**, *93*, 2325−2327. (b) Taxol is a registered trademark of Bristol-Myers Squibb Co., Princeton, NJ.

(2) Bissery, M.-C.; Guénard, D.; Guéritte-Voegelein, F.; Lavelle, F. *Cancer Res.* **1991**, *51*, 4845−4852.

(3) (a) Greco, F. A.; Thomas, M.; Hainsworth, J. D. *Cancer J. Sci. Am.* **1999**, *5*, 179−191. (b) Perez, E. A. *Semin. Oncol.* **1999**, *26*, 21−26. (c) McGuire, W. P.; Ozols, R. F. *Semin. Oncol.* **1998**, *25*, 340−348; *25*, 707.

(4) See, however: Snyder, J. P.; Nevins, N.; Cicero, D. O.; Jansen, J. *J. Am. Chem. Soc.* **2000**, *122*, 724−725.

(5) (a) Fenoglio, I.; Nano, G. M.; Vander Velde, D. G.; Appendino, G. *Tetrahedron Lett.* **1996**, *37*, 3203−3206. (b) Marder-Karsenti, R.; Dubois, J.; Bricard, L.; Guénard, D.; Guéritte-Voegelein, F. *J. Org. Chem.* **1997**, *62*, 6631−6637.

(6) (a) Gunatilaka, A. A. L.; Ramdayal, F. D.; Sarragiotto, M. H.; Kingston, D. G. I. *J. Org. Chem.* **1999**, *64*, 2694−2703. (b) Guénard, D.; Guéritte-Voegelein, F. Private communication.

(7) (a) Kingston, D. G.; Magri, N. F.; Jitrangsri, C. In *New Trends in Natural Product Chemistry*; Rahman, A., Quesne, L., Eds.; Elsevier: Amsterdam, 1986; Vol. 26, pp 219−235. (b) Samaranayake, G.; Magri, N. F.; Jitrangeri, C.; Kingston, D. G. I. *J. Org. Chem.* **1991**, *56*, 5114−5119. (c) Wahl, A.; Guéritte-Voegelein, F.; Guénard, D.; Le Goff, M.-T.; Potier, P. *Tetrahedron* **1992**, *48*, 6965−6974. (d) Chen, S.-H.; Huang, S.; Wei, J.; Farina, V. *Tetrahedron* **1993**, *49*, 2805−2828. (e) Baccatin oxetane ring opening was also reported previously: Guéritte-Voegelein, F.; Guénard, D.; Potier, P. *J. Nat. Prod.* **1987**, *50*, 9−18.

(8) Appendino, G.; Danieli, B.; Jakupovic, J.; Belloro, E.; Scambia, G.; Bombardelli, E. *Tetrahedron Lett.* **1997**, *38*, 4273−4276.

(9) Nicolaou, K. C.; Claiborne, C. F.; Nantermet, P. G.; Couladouros, E. A.; Sorensen, E. J. *J. Am. Chem. Soc.* **1994**, *116*, 1591−1592.

(10) Shintani, Y.; Tanaka, T.; Nozaki, Y. *Cancer Chemother. Pharmacol.* **1997**, *40*, 513−520.

(11) Klar, U.; Graf, H.; Schenk, O.; Röhr, B.; Schulz, H. *Bioorg. Med. Chem. Lett.* **1998**, *8*, 1397−1402.

(12) Wang, M.; Xia, X.; Kim, Y.; Hwang, D.; Jansen, J. M.; Botta, M.; Liotta, D. C.; Snyder, J. P. *Org. Lett.* **1999**, *1*, 43−46.

(13) Zbinden P.; Dobler, M.; Folkers, G.; Vedani, A. *Quant. Struct. Act. Relat.* **1998**, *17*, 122−130.

10.1021/jo9916075 CCC: $19.00
Published on Web 01/30/2000

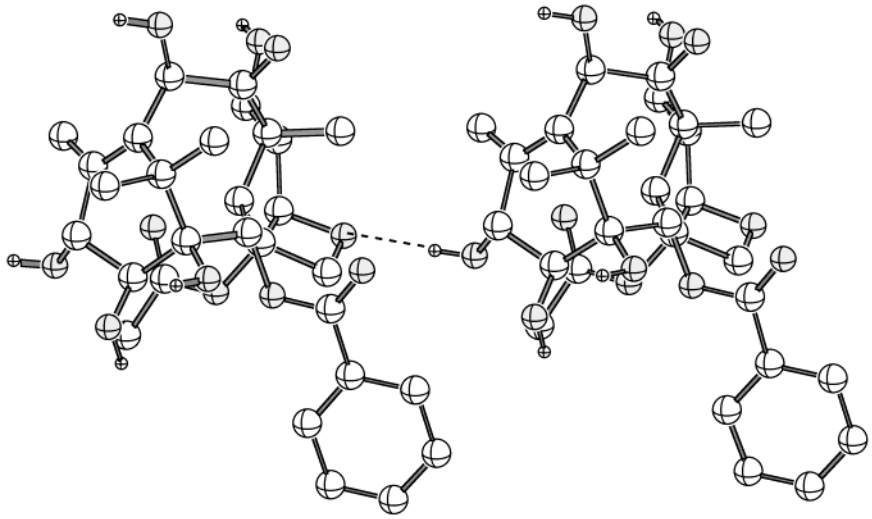

Figure 1. X-ray crystal structure of **3** illustrating the intermolecular hydrogen bond (1.82 Å) between the C-13 hydroxyl and the oxetane oxygen in adjacent molecules in the solid state. Oxygen atoms are darkened. The acetone molecules are not shown.

for the Taxol structure.[16] We conclude that both conformational and electrostatic effects are indeed manifested by the oxetane ring. However, it is also clear that an oxetane ring is not obligatory for a taxoid analogue to retain Taxol-like activity, at least as it pertains to microtubule assembly.

In the following, the reader will be presented with a number of computer-aided deductions and predictions. In each case, however, we have preceded minireceptor projections with analyses of known structures and their measured binding tendencies with respect to microtubule formation. Only where the minireceptor model succeeds in mapping the experiment do we extend its application to unknown structures. In certain cases, the structures under discussion are docked into the Taxol−tubulin binding site to elicit additional insights.

Oxetane Hydrogen Bonding

As a cyclic ether, the four-membered ring in Taxol is a potential hydrogen bond acceptor. Do oxetanes, in fact, engage in such noncovalent interactions? A search of the Cambridge Structural Database (CSD)[17] found 106 structures containing the oxacyclobutane ring. Nine of these involve the oxygen as a partner in intermolecular H-bonds or CO- - -HX dipole−dipole interactions ranging from 1.8 to 2.7 Å. One of the structures is 14-β-hydroxy-10-deacetylbaccatin III (**3**) cocrystallized with a molecule of acetone (not shown).[18]

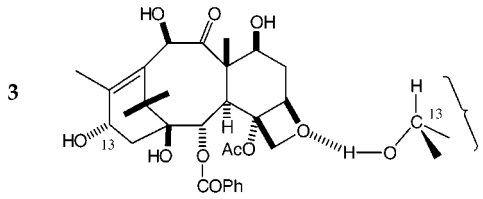

The compound exhibits a short hydrogen bond (1.82 Å) very near the plane of the oxetane ring but slightly displaced in the direction of C-7 and C-8 (φ(OH- - -OC_{20}) = 169°, Figure 1). Not surprisingly, the oxetane ring in Taxol likewise participates in hydrogen bonding to the β-tubulin protein. In this case, however, the protein delivers an OH from Thr276 to the four-ring face clearly syn to C-7 and C-8 (φ(OH- - -OC_{20}) = −86°).[14]

Thus, not only is the oxetane moiety able to sustain normal H-bonds, but the Taxol architecture places no constraints on the D-ring in its role as either a Brønsted or Lewis base. The latter has been demonstrated by transforming Taxol analogues to oxetane ring opened products upon treatment with more powerful electrophiles.[7,19] Notably, the D-ring hydrogen bonding capacity, in part, was inspirational in directing us to incorporate arginine as the oxetane H-bond donor in our second-generation Taxol−epothilone minireceptor.[12,16] In addition to the electrostatics associated with an X−H- - -oxetane hydrogen bond, the polar and rigidly oriented C−O bonds also engage in other productive electrostatic interactions with the surrounding protein. Both elements combine to make up the oxetane contribution to binding at its β-tubulin subsite.

(14) A novel T-shaped conformation of Taxol resides in the largely hydrophobic β-tubulin binding pocket: Snyder, J. P.; Nettles, J.; Cornett, B.; Downing, K.; Nogales, E. Submitted for publication.

(15) Nogales, E.; Wolf, S. G.; Downing, K. H. *Nature* **1998**, *391*, 199−203.

(16) The minireceptor model employed in the present work[12] was patterned after the nonpolar conformation of Taxol. Analogues of Taxol and epothilone were aligned and surrounded with 20 amino acid side chains taken from peptide fragments of β-tubulin determined by taxoid photoaffinity labeling studies. The geometry of the resulting surrogate receptor was refined under the constraint that ligand binding affinities could be estimated with high accuracy ($r \geq 0.99$; see Energetics below). The model sustains Taxol−minireceptor hydrogen bonds from C-1′ to C-3′ along the ligand's C-13 side chain and at the oxetane oxygen. Hydrophobic subsites surround the phenyl termini of C-2 and C-3′, and other side chains fill the gaps to create a protein-like binding pocket similar in many respects to the interactions found at the Taxol−β-tubulin binding center.[14] Insofar as the present study is concerned, the two models differ significantly in the oxetane H-bond donor; Arg for the minireceptor, Thr for the protein−ligand complex. The former was chosen prior to knowledge of the 3-D character of the β-tubulin structure. The next generation anti-tubulin minireceptor will rectify this and other points of difference.

(17) The Cambridge Structural Database: http://www.ccdc.cam.ac.uk/prods/csd.html.

(18) Appendino, G.; Gariboldi, P.; Gabetta, B.; Pace, R.; Bombardelli, E.; Viterbo, D. *J. Chem. Soc., Perkin Trans. 1* **1992**, 2925−2929.

(19) Farina, V.; Huang, S. *Tetrahedron Lett.* **1992**, *33*, 3979−3982.

Energetics of the Binding Model

The semiquantitative minireceptor model employed in the present work was constructed on the basis of microtubule assembly data encompassing both taxoids and epothilones.[12] To estimate relative ligand binding energies, the 3-D model uses a three-term scoring function (eq 1) adapted from the work of Blaney and co-workers and implemented in the PrGen software.[20,21]

$$\Delta G°_{calc} \approx \Delta E_{calc} - T\Delta S_{binding} - \Delta G_{solv,lig} \qquad (1)$$

The term ΔE_{calc} is the interaction energy between bound ligand and the minireceptor. In the PrGen context, it includes explicit van der Waals, electrostatic, and hydrogen bonding contributions. The remaining two terms are penalty terms associated with the migration of a ligand from an aqueous milieu into a constrained receptor cavity. $T\Delta S_{binding}$ accounts for the loss of torsional entropy for a flexible molecule during the binding process. It is estimated by identifying all freely rotatable bonds and deducting 0.7 kcal/mol for each of them.[22] $\Delta G_{solv,lig}$ accounts for the free energy of desolvation when the ligand binds. We have used the AM1/SM1 method[23] to obtain this quantity. It needs to be pointed out that a truly accurate assessment of solvation for a flexible molecule requires sampling the ensemble of conformations in solution. The corresponding Boltzmann-weighted energies provide the most accurate solvation free energy. In the present work, we estimate relative solvation energies by performing AM1/SM1 calculations only on the conformation of the ligand bound in the minireceptor. While approximate, this strategy is sufficient for producing excellent QSAR correlations in the minireceptor context.[12] When comparing individual structures, however, the numbers should be taken as qualitative rather than quantitative. In subsequent sections, the elements of eq 1 are used to assess calculated similarities and differences in the binding of Taxol to β-tubulin as reflected by the tendency of Taxol analogues to promote $\alpha\beta$ dimer polymerization to microtubules.

Oxetane Heteroatom Replacements

To date, the oxygen in ring-D of Taxol and baccatin congeners has been replaced with NH,[5] N-Ac,[5a] N-Bn,[5b] S,[6] and Se.[6a] None of the compounds are as effective as Taxol either in the microtubule assembly assay or in cell cytotoxicity bioassays.

As outlined in Table 1, the azadocetaxel analogue **4** is eight times less active than Taxol and 16 times less active than Taxotere in the microtubule (MT) assembly assay. For the exo and endo orientations of the azetidine NH bond, we predict tubulin dimer assembly similar to or slightly better than **1** and **2**, respectively. In addition, rigid docking of azataxoids **4** and **5** into the tubulin−Taxol model[14] (see the Computational Procedures) illustrates a sterically unencumbered association with the protein. The binding mode is not only identical to that of Taxol, but also the NH group forms a hydrogen bond to Thr276 analogous to the oxetane.

Table 1. Estimation of Binding and Solvation Energies for Oxetane O-Atom Replacements in Taxol and Taxotere Analogues

	X	$IC_{50}/IC_{50,TX}$	K_{pred}/K_{TX}[a]	$\Delta\Delta E_{calc}$[b]	$\Delta G_{solv,lig}$[b,c]
1	O	1	1	0.0	−14.7
2	O	0.5	0.1	−3.4	−12.9
4	NH	8	0.2, 0.2[d,e]	−4.8[e]	−14.3, −14.6
5	NH		0.4, 0.4[d,f]	−2.8[f]	−15.1, −16.1
6	S	≥6, 9	164[g]	10.6[g]	−13.5[h]
7	S	∼5i	6[e]	2.6[e]	−12.0
8	S		3[f]	2.3[f]	−14.2
9	CH_2		1[f]	1.7[f]	−13.4
10	CH_2		4[e]	3.9[e]	−11.6

[a] The predicted K_i's for Taxol and Taxotere are 2.9e−05 and 3.3e−06, while the experimental values are 1.5e−05 and 7.5e−06, respectively.[54] [b] From eq 1. [c] Aqueous free energies of solvation were obtained with AMSOL 5.4, AM1/SM1, using AMBER* optimized geometries. [d] Endo and exo NH bonds, respectively. [e] Relative to Taxotere. [f] Relative to Taxol. [g] Relative to 4-deacetyl-4-OCOOMe Taxol. [h] $\Delta G_{solv,lig}$ for the oxetane analogue of **6** is −13.6 kcal/mol. [i] Reference 6b.

	X	R_1	R_2	R_3
1	O	Ph	Ac	Ac
2	O	O-*t*-Bu	H	Ac
4	NH	O-*t*-Bu	H	Ac
5	NH	Ph	Ac	Ac
6	S	Ph	Ac	CO_2Me
7	S	O-*t*-Bu	H	Ac
8	S	Ph	Ac	Ac
9	CH_2	Ph	Ac	Ac
10	CH_2	O-*t*-Bu	H	Ac

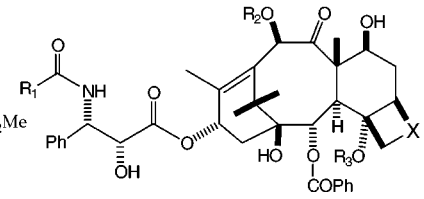

Where does the discrepancy between IC_{50}(rel) and prediction lie? At physiological or neutral pH in the presence of protein, the ring NH will be protonated. Our current minireceptor model is not equipped to handle a cationic center at this position. However, we calculate that the solvation energy (AM1/SM1) for protonated azadocetaxel **4** is 44 kcal/mol greater than the average of the exo/endo neutrals. Thus, we surmise that protonated **4**, despite a strong hydrogen bond to the protein, is too strongly solvated to permit effective migration from the aqueous milieu to the protein binding pocket relative to Taxol. The same property would reduce azadocetaxel's cytotoxic properties against cells guarded by a hydrophobic membrane bilayer. In agreement, **4** is completely inactive against the KB cell line.[5b]

The lowered activities for thietane analogues **6**−**8** are modeled semiquantitatively against experiment in Table 1. The 4-CO2Me derivative **6** is observed to be ≥6−9 times worse than the oxetane analogue depending on assay conditions,[6a] while the minireceptor method yields a ratio of 164. Thiataxotere **7** is deactivated relative to Taxotere by about a factor of 5,[6b] modeled here as a factor of 6. The activity of the unknown thiataxol **8** is predicted to be diminished to one-third of that for parent **1**. The reduced activities of the thiataxol analogues derive from a different source than the azataxoids. Free energies of solvation are calculated to be slightly lower than those of Taxol and Taxotere (0.1−0.9 kcal/mol, Table 1) in agreement with the 0.4 kcal/mol difference between dimethyl sulfide and dimethyl ether.[24] If anything, the solvation factor favors thietane binding.

(20) Blaney, J. M.; Weiner, P.; Dearing, A.; Kollman, P.; Jorgensen, E.; Oatley, S.; Burridge, J.; Blake, C. *J. Am. Chem. Soc.* **1982**, *104*, 6424−6434.
(21) Vedani, A.; Zbinden, P.; Snyder, J. P.; Greenidge, P. A. *J. Am. Chem. Soc.* **1995**, *117*, 4987−4994.
(22) (a) Andrews, P. R.; Craik, D. J.; Martin, J. L. *J. Med. Chem.* **1984**, *27*, 1648−1657. (b) Searle, M. S.; Williams, D. H. *J. Am. Chem. Soc.* **1992**, *114*, 10690−10697.
(23) Cramer, C. J.; Truhlar, D. G. *J. Am. Chem. Soc.* **1991**, *113*, 8305−8311; 9901.

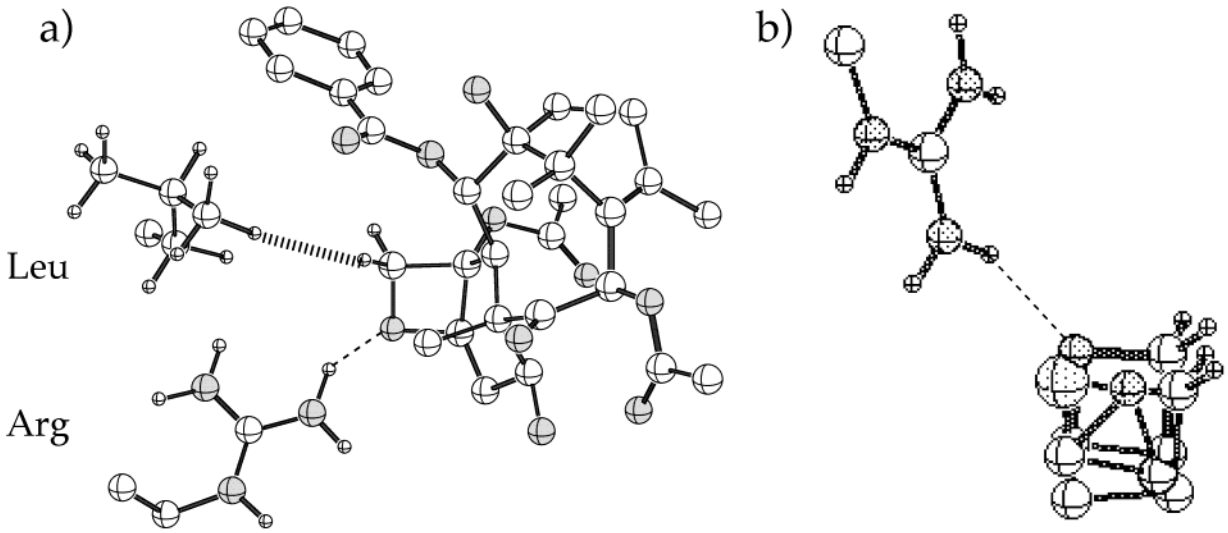

Figure 2. (a) Truncated Taxol in the minireceptor illustrating the Arg-oxetane H-bond (2.05 Å) and Leu-CH_2 H- - -H contact (2.39 Å). (b) Superposition of the oxetane, epoxide, and thietane rings from **1**, **8**, and **11** in the minireceptor showing that only the oxetane makes a classical hydrogen bond to Arg. Oxygen, nitrogen, and suflur atoms are darkened.

Within the minireceptor model, however, two significant differences are noted. First, the sulfur atom does not form a hydrogen bond to the nearby arginine side chain. Second, the four-membered ring, expanded in size by the relatively long C−S bonds, responds to unfavorable ligand−receptor interactions by backing further into the binding cavity (Figure 2b). The direction of the movement depends on the nature of the C-4 substituent (OCOMe or OCO_2Me). In either case, however, this movement diminishes productive ligand−protein interactions elsewhere in the binding site. A rough measure of the binding site energy change is indicated by $\Delta\Delta E_{calc}$ in Table 1, the predicted binding free energy minus the solvation and frozen torsion energy penalties. All of the sulfur-containing analogues are less satisfied in the binding cavity than **1** and **2**. Microtubule assembly capacity is thus predicted to decrease as observed. We have not modeled the selenium analogue, but a qualitative outcome similar to the sulfur analogues can be expected.

Finally, the oxetanes in **1** and **2** have been replaced by cyclobutane to give **9** and **10**, respectively. The latter are posited to be up to 40 times less effective at MT assembly than the parent drugs (Table 1). Like the sulfur analogues, they are more poorly solvated than the parent molecules. But unlike the sulfur-containing compounds, the relatively short C−C bonds avoid a steric clash between the C-21 methylene and the H-bond donor. The primary source of predicted reduction in activity comes from loss of favorable electrostatic interactions between β-tubulin and the four-membered ring. The oxetane binding site prefers polar C−X bonds that present properly oriented dipoles and hydrogen bonding capacity to the protein.

Modification of the oxetane ring by heteroatom replacement is thus seen to be a complex process involving aqueous solvation, protein−ligand electrostatics, and binding site steric effects. Clearly, the presence of a four-membered D-ring is not sufficient to guarantee optimal activity for Taxol analogues. In subsequent sections, we explore the consequences of alternative modifications of the oxetane ring as well as its removal.

Table 2. Estimation of Binding and Solvation Energies for Oxetane Ring Replacement and Deletion in Taxol Analogues

	X	$IC_{50}/IC_{50,TX}$	K_{pred}/K_{TX}	$\Delta\Delta E_{calc}$[a,b]	$\Delta G_{solv,lig}$[a,c]
1	O	1	1	0.0	−14.7
2	O	0.5	0.1	−3.4	−12.9
11	O		0.5	−2.7	−15.6
12	CH_2		0.6	−0.2	−13.9
13	(C═C)		1.4	0.3	−15.0
14	(C═CMe)		0.3	−2.3	−14.1
15	(C−C)		0.5	−0.2	−13.3

[a] From eq 1. [b] Relative to Taxol. [c] Aqueous free energies of solvation were obtained with AMSOL 5.4, AM1/SM1, using AMBER* optimized geometries.

Simple Ring Replacements

What are the consequences of maintaining rigidity in the C−D ring segment of Taxol, but altering its origin? Structures **11** and **12** substitute three-membered rings for the corresponding four rings in **1** and **9**. Remarkably, both the epoxide and the cyclopropane are predicted to be similar to Taxol in the microtubule assembly assay (Table 2). Epoxide **11**'s estimated β-tubulin binding affinity persists despite its higher solvation energy relative to **1**. While it does not form a hydrogen bond at the (C4, C5) oxygen, both electrostatic and van der Waals interactions are improved. The latter derives from the absence of an unfavorable oxetane C-20 CH_2−protein ligand interaction present in Taxol. In the minireceptor model, this takes the form of a Leu- - -CH_2 close contact (2.39 Å, Figure 2a). Within the binding pocket of β-tubulin, a similar interaction at 2.53 Å is observed between Leu217 and the same C-20 methylene.

The epoxidized molecule simply fits the binding pocket better than Taxol as indicated by the $\Delta\Delta E_{calc}$ in Table 2 and, thereby, compensates for the computed solvation disadvantage. Cyclopropane **12**, on the other hand, is less-well solvated than epoxide **11**. What the molecule loses in ligand−protein H-bonding and electrostatics upon O to CH_2 exchange, it makes up in its drive to move

(24) See the Supporting Information for: Hawkins, G. D.; Cramer, C. J.; Truhlar, D. G. *J. Phys. Chem.* **1996**, *100*, 19824−19839.

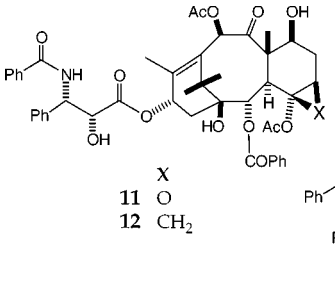

X
11 O
12 CH_2

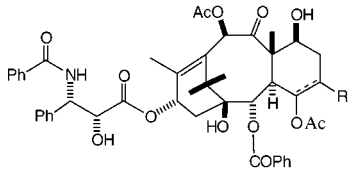

13 (C=C, R = H)
14 (C-C, R = Me)
15 (C-C, R = H)

out of solvent. At the same time, the smaller homologue escapes the unfavorable C-20 CH_2 steric encounter shown in Figure 2a. The net result is a rigid analogue predicted to be Taxol's match (Table 2). After this assessment, we learned that the CNRS research team has prepared the Taxotere analogue of **12**, 5(20)-deoxydocetaxel. Its tubulin binding affinity is half that of Taxotere and equivalent to that of Taxol.[6b,25]

Removal altogether of the oxetane ring as a formal CH_2═O elimination results in olefin **13**. This structural modification, among other things, relieves the potential protein−ligand steric clash depicted in Figure 2a. C-4 is modified from an sp^3 to an sp^2 center with the attendant variations in bond angles. Our expectation for this change was that the C-4 acetate would rotate up and out of the concave hydrophobic cavity and present itself at the edge of the molecule as depicted schematically by **13**. In fact, such an expectation goes unrealized in the minireceptor binding pocket. The fold of the B and C rings in the molecule is sustained by the trans stereochemistry at the ring junction. At the same time, the C4−C5 double bond asserts a rigidity for the fused A−C rings similar to a small D-ring, thus serving as a simple but effective conformational lock. As a result, the 4-OAc in **13** resides very close to its position in **1**. The molecule's binding affinity is predicted to be no more than a factor of 2 less than Taxol (Table 2). If this assessment is accurate, it suggests that a properly chosen substitutent at C-5 might well restore the full Taxol/Taxotere activity. Accordingly, structure **14** with a methyl at C-5 is suggested to enhance MT assembly by a factor of 5 relative to **13**.

Saturation of the double bond in **13** by delivery of H_2 from the less hindered β-face furnishes **15** with the C-4 OAc oriented α. The resulting C-ring chair cyclohexane with equatorial acetate is likewise forecast to be a Taxol binding mimic (Table 2). The C-4 acetate is tucked beneath the Taxol molecule and engages in hydrophobic clustering. No hydrogen-bonding equivalent of the oxetane oxygen is presented by the ligand. In the present model, saturation of the C-ring reduces solubility and thereby increases protein−ligand binding. The foregoing analyses set the stage for examination of Taxol derivatives in which the C or the D rings have been severed, namely, the seco-analogues.

D-Secotaxol Analogues

The Kingston group[7a,b] was the first to cleave the oxetane ring and to test the result for bioactivity. Thus, D-secotaxol **16**, prepared by exposure of **1** to Meerwein's reagent, proved to be at least 20 times poorer than Taxol in a tubulin depolymerization assay and inactive in a KB cell culture assay.[7b] These and related experiments prompted the argument that the oxetane ring is a necessity for activity.[26,27] The CNRS group, however, expressed the caveat that **16** lacks both an acetate at C-5 and the Taxol stereochemistry at C-5.[28]

(25) Dubois, J.; Thoret, S.; Guénard, D.; Guéritte, F. Submitted.

Table 3. Estimation of Binding and Solvation Energies for Oxetane Ring Cleavage Analogues: D-Secotaxol Analogues

	$IC_{50}/IC_{50,TX}$	K_{pred}/K_{TX}[a]	$\Delta\Delta E_{calc}$[b]	$\Delta G_{solv,lig}$[c]
1	1	1	0.0	−14.7
16	>21	5	−2.0	−17.8
17		2	1.6	−14.1
18		1	−0.6	−14.8
19		3	2.4	−13.8
20		0.9	−3.5	−15.9
21		1	−3.6	−14.7
22		0.5	−5.4	−16.3

[a] Relative to Taxol. [b] From eq 1. [c] Aqueous free energies of solvation were obtained with AMSOL 5.4, AM1/SM1, using AMBER* optimized geometries.

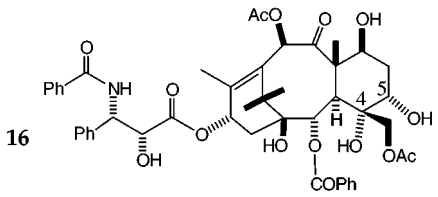

16

Very recently, ^1H NMR analysis of **16** in $CDCl_3$ has revealed that D-ring opening transmits a significant conformational change to the A-ring and a lesser one to the B-ring,[29] a result anticipated by Kingston.[7a] Specifically, the distorted boat conformer in Taxol becomes a pseudoenvelope in D-secotaxol. In turn, the C-13 side chain is tucked further under the concave cavity of the molecule, and the 2-benzoyl group is displaced somewhat from its location in Taxol. One might tentatively conclude that the reshaping of **16** relative to **1** is the genesis of the reduced activity.

The minireceptor model posits that **16** is five times less effective than **1** in fair agreement with observation (Table 3). The form that resides in the binding pocket possesses a chair cyclohexane C-ring and is very similar in conformation to that determined by NMR.[29] An intriguing aspect of the calculation, however, is that the drop in binding is *not* due to oxetane ring opening. By the rough standard of $\Delta\Delta E_{calc}$, D-secotaxol enjoys a somewhat better overall protein−ligand interaction than Taxol (Table 3). In the minireceptor context, the binding pocket is sufficiently large and forgiving that it can tolerate a variety of taxoid and epothilone variations.[12] D-Secotaxol is no exception. Once bound, it is a welcome guest. The

(26) Kingston, D. G. I. In *Taxane Anticancer Agents*; Georg, G. I., Chen, T. T., Ojima, I., Vyas, D. M., Eds.; ACS Symposium Series 583; American Chemical Society: Washington, DC, 1995; pp 207−208.

(27) Chen, S.-H.; Farina, V. In *Taxane Anticancer Agents*; Georg, G. I., Chen, T. T., Ojima, I., Vyas, D. M., Eds.; ACS Symposium Series 583; American Chemical Society: Washington, DC, 1995; pp 257−259.

(28) Guéritte-Voegelein, F.; Guénard, D.; Dubois, J.; Wahl, A.; Marder, R.; Müller, R.; Lund, M.; Bricard, L.; Potier, P. In *Taxane Anticancer Agents*; Georg, G. I., Chen, T. T., Ojima, I., Vyas, D. M., Eds.; ACS Symposium Series 583; American Chemical Society: Washington, DC, 1995; pp 195−197.

(29) Boge, T. C.; Hepperle, M.; Vander Velde, D. G.; Gunn, C. W.; Grunewald, G. L.; Georg, G. I. *Bioorg. Med. Chem. Lett.* **1999**, *9*, 3041−3046.

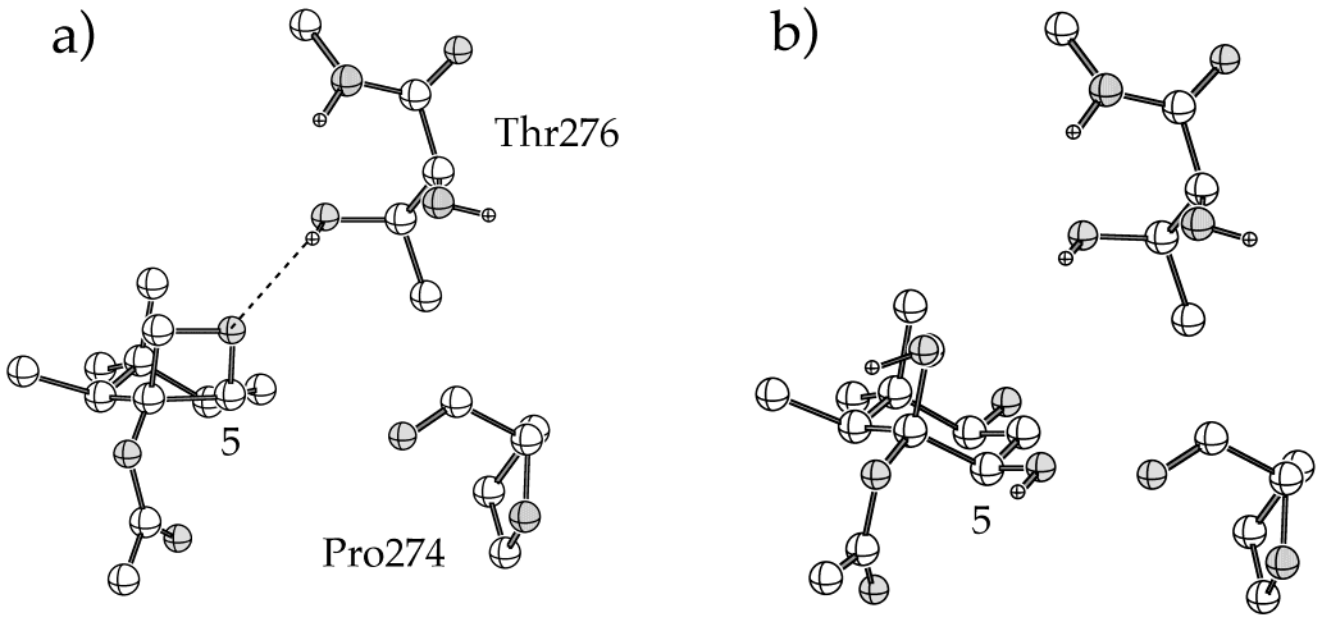

Figure 3. View of the β-tubulin binding subsite in the vicinity of Taxol's oxetane ring and the protein's Thr276: (a) Taxol oxetane hydrogen bonds to Thr276; (b) chair C-ring of **20** surrounded by the closest polar residues of tubulin. The OH groups of structures **20** and **22** appear to engage the protein by means of electrostatic interactions rather than by the shorter range hydrogen bonds. Oxygen and nitrogen atoms are darkened.

favorable ligand protein interaction results from the binding site's attempt to accommodate the new acetate emanating from C-20. While the C=O of the latter makes a hydrogen bond to Arg as does oxetane in **1**, structure **16** shifts slightly in the binding pocket and establishes favorable C-1′ C=O and C-3′ NH hydrogen bonds.

Despite these microevents, the desolvation energy for **16** (17.8 kcal/mol) is the largest value in Tables 1−3, even larger than for unprotonated azataxol (16.0 kcal/mol). This result is clearly a consequence of the presence of two hydroxyl groups at C-4 and C-5 and the exposure of the C-4 CH_2 OAc moiety to solvent. On a relative scale, compound **16** is unusually reluctant to leave the aqueous phase. This property would seem to govern its biobehavior.

We were interested in whether relocation of acetate and a switch in configuration at C-4 and C-5 in **16** might lead to further insights into the importance of the oxetane ring for taxoid activity. Consequently, we examined the estimated binding affinities for the unknown structures **17**−**22**, all of which employ chair cyclohexanes in ring C.

	R_1	R_2	R_3
17	CH_3	OH	H
18	H	OH	H
19	H	OCH_3	H
20	CH_2OH	OH	H
21	CH_2OH	H	H
22	CH_2OH	H	OH

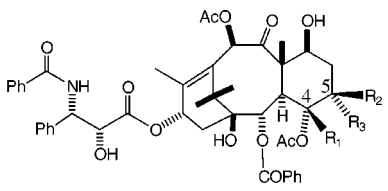

Indeed, with C-4 OAc located α, all of the structures are suggested to be superior to **16**. Two variations bearing a single OH group on or near C-4 and C-5 (**18** and **21**, Table 3) are potential biomimetic equivalents of **1**. Their scoring results from a combination of favorable electrostatic and steric effects. Two additional structures with a pair of OH moieties in this vicinity are epimeric at C-5 (**20** and **22**). Both are evaluated to be potent competitors of Taxol. Several conformations of the substituents at C-4 and C-5 in structure **20** were considered. The lowest energy form that did not involve multiple intramolecular hydrogen bonds was chosen as representative. It is predicted to benefit from both tight binding to the minireceptor ($\Delta\Delta E_{calc}$) and a modest solvation energy. It is perhaps noteworthy that the somewhat shielded C-5 α-OH in epimer **22** engenders a lower solvation penalty than the corresponding β-OH in **20**, while experiencing increased ligand−minireceptor interaction. The reader is reminded, however, that we are working with single-conformer solvation estimates. The numbers in the tables should therefore be taken as more qualitative than quantitiative. Nonetheless, one interesting projection of the analysis is that tubulin binding is predicted to be insensitive to configuration at C-5 for epimers **20** and **22**.

D-Seco analogue **16** can be docked at the modeled tubulin−taxoid binding site[14] as can **20** and **22** (see the Computational Procedures for docking details). The latter two structures conform to the lipophilic pocket by presenting their terminal C-2 and C-3′ phenyl rings and the C-4 acetate methyl in the same binding subsites as occupied by the corresponding hydrophobes of **1.** The important C-2′ OH hydrogen bond is likewise retained. In the ring-D subsite, however, the alignments of oxygen functionalities at C-4 and C-5 differ from that of the oxetane ring. Neither structure exhibits a hydrogen bond to the protein's Thr276. Figure 3 depicts the environment around C-4 and C-5 and illustrates how the hydroxylated C-ring chair in **20** compares in spatial disposition to the four-membered ring of Taxol.

C-Secotaxol Analogues

While cleavage of Taxol's oxetane ring is one means of testing the moiety's function at the microtubule binding site, depriving it of its A−C ring rigidifying influence and providing it with the freedom to move relative to the rest

Table 4. Estimation of Binding and Solvation Energies for C-Secotaxol Analogues

	$IC_{50}/IC_{50,TX}$[a]	$IC_{50}/IC_{50,TX}$[b]	K_{pred}/K_{TX}[c]	$\Delta\Delta E_{calc}$[d]	$\Delta G_{solv,lig}$[e]
1	1	1	1	0.0	−14.7
2	0.3	0.3	0.1	−3.4	−12.9
23	0.5	0.03	0.005	−10.0	−12.4
24	2	2	0.1	−6.5	−13.7
25	112	>4	5	1.2	−15.1

[a] Relative to Taxol (2.5 nM) in MDA-MB321 breast cancer; ref 24. [b] Relative to Taxol (2600 nM) in adriamycin-resistant MCF-7 ADRr breast cancer cells; ref 30. [c] Relative to Taxol in the minireceptor tubulin polymerization assay. [d] From eq 1. [e] Aqueous free energies of solvation were obtained with AMSOL 5.4, AM1/SM1, using AMBER* optimized geometries.

of the molecule is another. Appendino and co-workers' discovery that oxidation of 10-deacetylbaccatin III at C-10 yields a 9,10-diketo derivative that rearranges by cleavage of the C7−C8 bond has furnished such a compound. Several steps of chemical manipulation on the ring-opened baccatin led to C-secotaxols **24** and **25**.[30] The first is related to compound **23**, 3′-dephenyl-3′-*i*-Bu-10-acetyltaxotere,[31] while the second is a congener of Taxol (**1**).

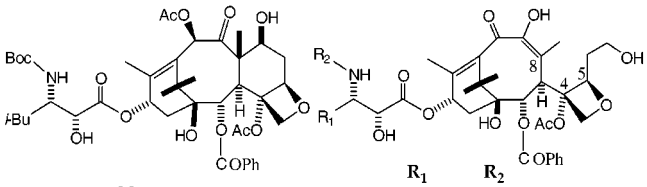

	R_1	R_2
24	*i*-Bu	Boc
25	Ph	Bz

Compound **23** is a somewhat more cytotoxic agent than Taxol and Taxotere (Table 4).[30,31] In addition, the substance has been reported to exhibit very low toxicity in nude athymic mice.[32] Remarkably, activity in the C-seco variants is not only retained, but is dependent on the distal C-13 hydrophobes R_1 and R_2.[30,33] While the C-seco analogue **24** drops to an activity of one-fourth, it is still just half as efficacious as Taxol. By contrast, the Taxol derivative **25** loses more than 2 orders of magnitude of cell killing power in at least one normal cell line. Although the dataset is not large, replacement of the two terminal C-13 phenyls in the oxetane series with alkyl groups (**1** → **23**) causes only a moderate change in activity. The situation is reminiscent of the general trend in Taxol and Taxotere alkyl derivatives,[31,34] although much larger changes are often observed for drug-resistant cell lines.[30,35] In the C-seco series, however, substitution of two phenyls with two alkyl groups (**25** → **24**) appears to exert an exceptional beneficial influence with respect to toxicity (Table 4). Why is this?

We begin the analysis with the observation that published data on **23**−**25** are, with one exception, derived from cell cytotoxicity measurements. By comparison, our minireceptor model is based on microtubule assembly data. While both types of assays are often run for a series of compounds, the correlation is not always linear. Since membrane passage and other pharmacokinetic effects associated with living cells are not taken into account in simple QSAR models, the minireceptor protocol cannot be expected to map the data accurately. Consequently, for the C-seco analogues, we seek to model the trends in a completely qualitative sense.

Dialkyl compound **23** with an intact C-ring is calculated to be considerably more active than either Taxol or Taxotere in agreement with observation (Table 4). Decreased solvation plays a part, as anticipated by the fact that the phenyl group is solvated by 3.2 kcal/mol more than the butyl group.[36] The major effect for **23**, however, is the substantial predicted increase in binding relative to **1** ($\Delta\Delta E_{calc}$, Table 4). Though both molecules engage in H-bonding from the oxetane rings, inspection of the minireceptor cavity illustrates that the *i*-Bu/*t*-Bu combination in **23** causes small movements in the vicinity of the C-13 side chain by comparison with Taxol. These promote numerous favorable electrostatic interactions including strengthened hydrogen bonds from C-1′ C═O and C-3′ NH.

We are now in a position to speculate on the remarkable cytotoxicity disparity between **24** and **25**. First we compare the oxetane-containing systems **1**, **2**, and **23**. In the Taxol−protein model, the docked compounds are essentially superimposable in the sense that all important functional groups occupy similar spatial positions consistent with a common and high cytotoxic potential against tumor cells (Table 4). Each of the three oxetane rings makes a hydrogen bond to Thr276 (Figures 3a and 4). Structure **24**, when flexibly docked, situates its C-2, C-4, and C-3′ hydrocarbon termini in the same subsites as the corresponding centers in **1**, **2**, and **23**. In contrast, the less constrained oxetane ring is displaced from that in the rigid structures. The 2−3 Å movement, however, does not eliminate an H-bond to Thr276.

The situation is depicted in Figure 4b, which shows a superposition of the four-membered rings in the oxetane subsite. As mentioned previously, Taxol's oxetane oxygen accepts an OH interaction from the face of the ring syn to C-8. Structure **24** likewise serves as a hydrogen-bond acceptor, but from the opposite "anti" face of the ring. The threonine OH resides in a center that formally bisects the location of the oxetane oxygens of the two compounds. Simple rotation around the CαCβ−OH bond provides access to both oxygens.

When flexibly docked, the C-ring-opened Taxol analogue **25** retains an oxetane location as illustrated in Figure 4b. It likewise shows a good spatial disposition for C-2 and C-3′ phenyls as well as the C-4 methyl. Different, however, are the torsional angles from C-13 to C-3 relative to their values in **1**, **2**, **23**, and **24**. The C-2′ OH hydrogen bond is lost, and the C-1′ carbonyl is displaced so as to engage in a different set of polar ligand−protein interactions in this region of the binding pocket. The relative mispositioning of C-1′/C2′ functionality is consistent with the positive $\Delta\Delta E_{calc}$ in Table 4. In

(30) Appendino, G.; Danieli, B.; Jakupovic, J.; Belloro, E.; Scambia, G.; Bombardelli, E. *Terahedron Lett.* **1997**, *38*, 4273−4276.
(31) Ojima, I.; Duclos, O.; Kuduk, S. D.; Sun, C.-M.; Slater, J. C.; Lavelle, F.; Veith, J. M.; Bernacki, R. J. *Bioorg. Med. Chem. Lett.* **1994**, *4*, 2631−2634.
(32) Bombardelli, E.; Riva, A. In *Virtual Activity, Real Pharmacology*; Verotta, L., Ed.; Research Signpost: Trivandrum 1997; pp 61−83.
(33) Distefano, M.; Scambia, G.; Ferlini, C.; Gallo, D.; De Vincenzo, R.; Filippini, P.; Riva, A.; Bombardelli, E.; Mancuso, S. *Anti-Cancer Drug Des.* **1998**, *13*, 489−499.
(34) (a) Boge, T. C.; Himes, R. H.; Vander Velde, D. G.; Georg, G. I. *J. Med. Chem.* **1994**, *37*, 3337−3343. (b) Ojima, I.; Kuduk, S. D.; Pera, P.; Veith, J. M.; Bernacki, R. J. *J. Med. Chem.* **1997**, *40*, 279−285.
(35) Ojima, I.; Slater, J. C.; Pera, P.; Veith, J. M.; Abouabdellah, A.; Bégue, J.-P.; Bernacki, R. J. *Bioorg. Med. Chem. Lett.* **1997**, *7*, 133−128.

(36) The free energies of aqueous solvation for benzene and 2-methylpropane are −0.87 and 2.3 kcal/mol, respectively; cf. ref 22.

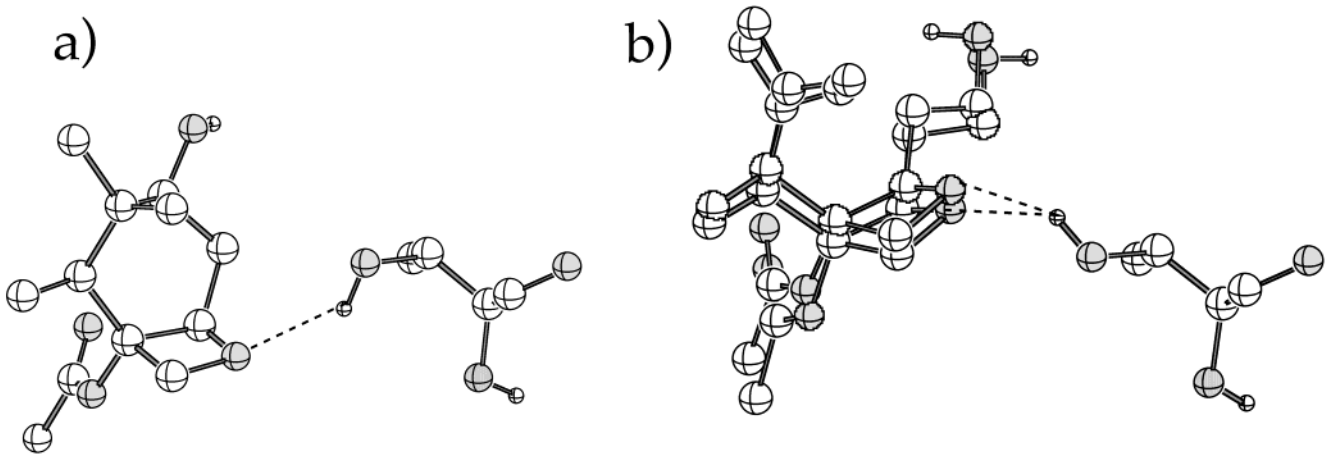

Figure 4. Interaction of oxetane rings with Thr276 in the oxetane subsite of the Taxol−tubulin binding pocket: (a) **1**; (b) **24** and **25**. Rotation about Cβ-O(H) in Thr276 allows a hydrogen bond to be established at either position of the oxetane oxygen. Oxygen and nitrogen atoms are darkened.

addition to an apparent unfavorable overall binding interaction with the protein, compound **25** suffers from a raised solvation energy (−15.1 kcal/mol) relative to all other compounds listed in Table 4. In stark contrast, compound **24** exhibits just the opposite properties computationally. The two alkyl groups not only assist driving the molecule out of the water and into the protein ($\Delta G_{solv,lig} = -13.7$ kcal/mol), but they also contribute to a much tighter ligand−protein complex with origins similar to those described for **23**.

The effect of the alkyl groups is a delicate one that deserves further study. One wonders, for example, how changes in size and shape of the alkyl group at C-3′ might influence the series SAR. Replacement of the Boc group in **24** with *n*-Hex is one variation that retains the cytotoxic activity of the system.[30] Conformational reorganization along the polar part of the C-13 side chain and the origin of its influence on binding also requires a deeper analysis.

Absence of D-Ring or a D-Ring Equivalent

Recently, several efforts have been made to eliminate the D-ring altogether.[9,11,37] A notable result is the preparation of compound **26** in which ring C has been simplified to a benzene ring.[9] The substance shows significant activity against a variety of tumor cell lines ranging from 1 to 0.0001 times as effective as Taxol, while a diastereomer exhibits no cytotoxicity under the same conditions. Regrettably, the tubulin assembly assay was not performed for this compound.[38] Consequently, we are obliged to assume that **26** poisons cells by a mechanism analogous to that of Taxol. In an attempt to rationalize the bioresults for the compound, we performed a conformational analysis seeking variation in ring B. While many side-chain conformations were obtained, only a single eight-membered ring conformation identical to the X-ray structure of a truncated analog[9] was located. The tricyclic core is acutely folded such that the methyl at C-12 resides over the annelated benzene ring. It would appear that, like the C-ring double bond in **14**, a B-ring double bond between C-3 and C-8 serves as a conformational lock for the remaining system as well.

Assuming that **26** and **1** bind at a common tubulin site, the appropriate side chain conformer was superimposed on the minireceptor Taxol structure and evaluated for tubulin binding affinity. The best match yields a structure predicted to bind with the same affinity as **1**. The cup-shaped structure, lacking an equivalent of the oxetane oxygen for H-bonding, slides deep into the binding pocket to make electrostatic and hydrophobic contacts in character and strength very similar to Taxol.

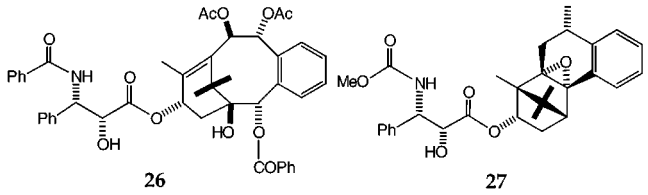

26 **27**

Compound **27** is another Taxol mimic lacking an oxetane equivalent that stabilizes microtubules at a level comparable to Taxol.[11] Minireceptor evaluation underestimates the compound's microtubule stabilizing capacity to be 2.7 times less active than the latter. Unfortunately, unusually high concentrations are needed to inhibit cell growth. In this respect, the oxetane-depleted compounds **26** and **27** are similar. Since compound **27** can penetrate the cell membrane, reach the nucleus, and condense microtubules in whole cells,[39] Klar and coworkers have suggested[11] that the diminished cytotoxicity relative to Taxol is due to the fact that Taxol and certain analogues exert their effects both by microtubule stabilization and by additional mechanisms that block tumor cell growth. The induction of gene expression[40] and Taxol-mediated inhibition of the anti-apoptotic protein Bcl-2[41] are two of the possibilities previously raised in this respect. A recent dissenting viewpoint, however, argues that all clinically relevant cytotoxicity of Taxol is associ-

(37) (a) Blechert, S.; Kleine Klausing, A. *Angew. Chem., Int. Ed. Engl.* **1991**, *30*, 412−414. (b) Blechert, S.; Jansen, R.; Velder, J. *Tetrahedron* **1994**, *50*, 9649−9656.

(38) Nicolaou, K. C. (Scripps Institute), private communication.

(39) Klar, U. (Schering AG), private communication.

(40) (a) Kirikae, T.; Ojima, I.; Kirkae, F.; Ma, Z.; Kuduk, S. D.; Slater, J. C.; Takeuchi, C. S.; Bounaud, P.-Y.; Nakano, M. *Biochem. Biophys. Res. Comm.* **1996**, *227*, 227−235. (b) Lee, L.-F.; Haskill, J. S.; Mukaida, N.; Matsushima, K.; Ting, J. P.-Y. *Mol. Cell. Biol.* **1997**, *17*, 5097−5105. (c) Moos, P. J.; Fitzpatrick, F. A. *Proc. Natl. Acad. Sci. U.S.A.* **1998**, *95*, 3896−3901.

ated with the compound's tubulin-binding properties.[42] If such turns out to be the case, substance **27** may be a better substrate for Pgp (P-glycoprotein) and MRP (multidrug resistance protein) drug efflux pumps than Taxol itself.[43] Whatever the outcome of the continuing investigations, presumably compound **26** acts analogous to **27** in its cytotoxic actions.

Conclusions

Oxetane rings embedded in a variety of molecular frameworks engage in hydrogen bonding in the solid state. Baccatin **3** represents the taxoid family. The phenomenon extends to Taxol (**1**) at the β-tubulin binding site.[14] The latter was anticipated by our first- and second-generation Taxol minireceptor models in which an arginine was incorporated as the H-bonding anchor for the oxygen of the four-membered ring.[12,44] These empirical and computational observations support the general belief that one of the essential features of Taxol analogue SAR is the presence of an oxetane ring at C4−C5 in the molecule and that it operates by imparting a productive noncovalent interaction with the tubulin protein. Despite the oxetane's capacity to form hydrogen bonds, these are known to be somewhat weaker than those to a carbonyl group and nondirectional with respect to the oxygen lone pairs in a 3-D wedge roughly perpendicular to the plane of the C−O−C unit.[45,46] Consequently, it can be expected that certain Taxol analogues will form a hydrogen bond, but bind only weakly. Compound **25** is a case in point (Figure 4). Others may not form such a noncovalent contact, but still bind the protein effectively. Stuctures **11**, **12**, **20,** and **22**, for example, are predicted to fall in this category. Removal of the hydrogen bonding functionality altogether as in **26** and **27** may be deleterious to cell killing but not necessarily to protein binding.

Several structures considered in this work address the second issue regarding the role of the oxetane ring: rigidification of the fused A−C ring system. Oxetane surrogates, for example three-membered rings (**11** and **12**) and an appropriately placed double bond (**13** and **14**), likewise furnish a high degree of structural stiffness and are predicted to maintain Taxol-like protein polymerization activity. The principle extends to benzannulated **26**, which hampers B-ring conformational mobility by placement of a double bond at C3−C8. Rigidity does not appear to be obligatory for predicted or actual activity, however. The potentially mobile cyclohexane C-ring analogues **15**, **20**, and **22** are illustrative. Appendino's C-seco analogue **24** lacking the C-ring is yet another variant that incorporates an important element of conformational freedom unavailable to analogues of **1** and **2**, yet retains impressive microtubule assembly and cell cytotoxicity properties.[30,33] While the notion that oxetane conformational locking is expendable has yet to be demonstrated persuasively by experiment, the structural and biological predictions for a variety of structural types along with the data for **24** are suggestive that rigidification is neither an absolute nor a strong requirement for taxoid activity.

In sum, the oxetane ring in Taxol congeners is capable of making a positive contribution to the bioactivity both in terms of hydrogen bonding and A−C ring rigidification. However, it would appear that while these elements are sufficient to support Taxol-like activity, they are by no means necessary. This conclusion in part is reached by using a second generation Taxol minireceptor model[12] in a predictive mode. An important feature of the model is the explicit introduction of ligand solvation as a critical element in assessing tubulin binding and subsequent microtubule assembly. Not all of our projections are likely to prove accurate. The activity of a number of structures may well be overpredicted as seems to be the case for **2** and **23**. While we intend to improve the predictive aspects in a third generation model, we believe the current protocol to be sufficiently sound to suggest that the oxetane ring should be unseated as an essential ingredient of Taxol SAR. In this spirit, it can be anticipated that simple D-seco Taxol analogues as well as those lacking the oxetane ring will be synthesized and shown to carry activity equivalent to that of Taxol and Taxotere.

Computational Procedures

K_i predictions were peformed with the PrGen suite of programs.[13,21,47] Structures to be evaluated were constructed in MacroModel 5.5[48] and optimized to the nearest local minimum with AMBER*/GBSA/H_2O.[49] ESP (electrostatic potential) charges were subsequently calculated by employing MOPAC6.[50] Solvation energies were obtained with AMSOL5.4 AM1-SM1.[23] The structures were fitted to the minireceptor conformation of Taxol by means of the SEAL procedure[51] and then transferred to the minireceptor model. Since the latter has been tailored by extensive training and test sets, only the new ligand structure is optimized with the Yeti force field within the minireceptor binding site. The resulting K_i prediction is based on the ligand−receptor interaction, ligand desolvation, and entropy compensation as described by eq 1. The present calculations and the first generation Taxol minireceptor model do not explicitly include the internal energy change of the ligand before and after docking.

Docking experiments described herein employed the program DOCK 4.0.1[52] and a recently developed Taxol−tubulin

(41) (a) Aime-Sempe, C.; Kitada, S.; Reed, J. C. *Blood* **1996**, S-1, *88*, 805. (b) Leiu, C. H.; Chang, Y.-N.; Lai, Y.-K. *Biochem. Pharmacol.* **1997**, *53*, 1587−1596. (c) Rodi, D. J.; Janes, R. W.; Sanganee, H. J.; Holton, R. A.; Wallace, B. A.; Makowski, L. *J. Mol. Biol.* **1999**, *285*, 197−203.

(42) Blagosklonny, M. V.; Fojo, T. *Int. J. Cancer* **1999**, *83*, 151−156.

(43) (a) Shapiro, A. B.; Ling, V. *Acta Physiol. Scand. Suppl.* **1998**, *643*, 227−234. (b) Eytan, G. D.; Kuchel, P. W. *Int. Rev. Cytol.* **1999**, *190*, 175−250. (c) Hendrikse, N. H.; Franssen, E. J.; van der Graaf, W. T.; Vaalburg, W.; de Vries, E. G. *Eur. J. Nucl. Med.* **1999**, *26*, 283−293.

(44) (a) Preliminary studies on a common pharmacophore for Taxol, epothilone B, and discodermolide were presented at the Alfred Benzon Symposium 42, Copenhagen, Denmark, June 8−12, 1997; Snyder, J. P. Abstracts. (b) Jansen, J. M.; Koehler, K. F.; Hedberg, M. H.; Johansson, A. M.; Hacksell, U.; Nordvall, G.; Snyder. J. P. *J. Chem. Inf. Comput. Sci.* **1997**, *37*, 812−818. (c) Snyder, J. P.; Xia, X.; Schestopol, M. A.; Kim, Y.; Bray, D.; Cain, M.; Liotta, D.; Koehler, K. F.; Jansen, J. M. In *Rational Molecular Design in Drug Research*; Liljefors, T., Jørgensen, F. S.,Krogsgaard-Larsen, P., Eds.; Munksgaard: Copenhagen, 1998; pp 115−135.

(45) Murray-Rust, P.; Glusker, J. P. *J. Am. Chem. Soc.* **1984**, *106*, 1018−1025.

(46) Lommerse, J. P. M.; Price, S. L.; Taylor, R. *J. Comput. Chem.* **1997**, *18*, 757−774.

(47) The current version of the software is PrGen 2.0.

(48) MacroModel web site: http://www.schrodinger.com/macromodel.html

(49) Still, C. W.; Tempczyk, A.; Hawley, R. C.; Hendrickson, T. *J. Am. Chem. Soc.* **1990**, *112*, 6127−6129.

(50) Stewart, J. J. P. MOPAC 6.0, Quantum Chemistry Program Exchange (QCPE), 455, Indiana University, Bloomington, IN 47405; http://www.chem.indiana.edu/qcpe.htm.

(51) (a) Kearsley, S. K.; Smith, G. M. *Tetrahedron Comput. Methodol.* **1990**, 3, 615−633. (b) Klebe, G.; Mietzner, T.; Weber, F. *J. Comput.-Aided Mol. Design* **1994**, 8, 751−778.

binding pocket model.[14] Individual analogue structures were generated by modifying the tubulin-bound Taxol structure in MacroModel 5.5 followed by geomety optimization with MMFF94[53] and the GB/SA water solvation model. The scoring grid consisted of 1 696 057 grid points distributed inside an 8 Å sided box centered on the Taxol binding site, corresponding to a grid-spacing of 0.25 Å. DOCK's grid-based scoring function is optimized for speed over accuracy and includes neither solvation nor entropy. Consequently, the program's ability to comparatively score different binding modes is semiquantitiative at best. The azataxoids **4** and **5** with the Taxol conformation were docked rigidly into the β-tubulin binding site. All other structures treated by the program were docked flexibly; i.e., all side chain torsions were allowed to vary. For each ligand examined with the flexible DOCK procedure, multiple runs at different sampling levels and random seed values were performed to minimize the chance of overlooking a favorable binding orientation.

Acknowledgment. We are grateful to Drs. Daniel Guénard and Francoise Guéritte-Voegelein (CNRS, Gif sur Yvette), Prof. Gunda Georg (University of Kansas), and Dr. Ulrich Klar (Schering AG) for sharing unpublished data and to Prof. Giovanni Appendino (Torino) and David Kingston (Virginia Polytechnic Institute) for stimulating discussions. Finally, we express our appreciation to Drs. Eva Nogales and Ken Downing for providing the coordinates of the $\alpha\beta$ tubulin dimer to us.

JO9916075

(52) Ewing, T. J. A.; Kuntz, I. D. *J. Comput. Chem.* **1997**, *18*, 1175−1189.

(53) Halgren, T. A. *J. Comput. Chem.* **1996**, *17*, 490−519; 520−552; 553−586; 616−641. Halgren, T. A.; Nachbar, R. B. *Ibid.* **1996**, *17*, 587−615.

(54) Nicolaou, K. C.; Winssinger, N.; Pastor, J.; Ninkovic, S.; Sarabia, F.; He, Y.; Vourloumis, D.; Yang, Z.; Li, T.; Ginnakakou, P.; Hamel, E. *Nature* **1997**, *387*, 268−272.